J. Chem. Sci. Vol. 126, No. 4, July 2014, pp. 967–973.

Combustion synthesis of cadmium sulphide nanomaterials for efficient visible light driven hydrogen production from water

A DAYA MANI[a], N XANTHOPOULOS[b], DANIELE LAUB[b] and C H SUBRAHMANYAM[a,*]

[a]Department of Chemistry, Indian Institute of Technology (IIT), Hyderabad, Yeddumailaram 502 205, India
[b]Ecole Polytechnique Federale de Lausanne (EPFL), CH-Lausanne, Switzerland
e-mail: csubbu@iith.ac.in

MS received 29 October 2013; revised 7 January 2014; accepted 6 February 2014

Abstract. Anion-doped cadmium sulphide nanomaterials have been synthesized by using combustion method at normal atmospheric conditions. Oxidant/fuel ratios have been optimized in order to obtain CdS with best characteristics. Formation of CdS and size of crystallite were identified by X-ray diffraction and confirmed by transmission electron microscopy. X-ray photoelectron spectroscopy confirmed the presence of C and N in the CdS matrix. The observed enhanced photocatalytic activity of the CdS nanomaterials for the hydrogen production from water (2120 μmol/h) can be attributed to high crystallinity, low band gap and less exciton recombination due to the C and N doping.

Keywords. Cadmium sulphide; combustion synthesis; anion doping; water splitting; H_2 production.

1. Introduction

Emission of oxides of carbon due to combustion of fossil fuels has made global warming a difficult task to handle.[1] As fossil fuel reserves are also depleting, there is an immediate need to look for renewable and/or clean energy sources that are free of carbon. In this context, research on direct utilization of solar energy has been increasing.[2] It is believed that in future, hydrogen may supersede the current non-renewable resources.[3,4] Traditional steam-methane reforming for hydrogen production is not an environment-friendly method and there is an immediate need to look for eco-friendly alternatives. Among the several methods for hydrogen production,[5–7] photocatalytic water splitting is gaining much attention due to its sustainable and environmentally benign nature.[8] However, the design of suitable materials that are active under sunlight still remains a challenge.

Among the materials available for harnessing solar energy, semiconductor nanostructures are gaining importance owing to their unique optical, electronic and catalytic properties. Cadmium sulphide (CS) with a direct band gap of 2.4 eV is one of the first semiconductors to be discovered. It is perhaps one of the most important electronic and optoelectronic materials with proven applications in solar cells, nonlinear optical devices and electronic devices.[9–11] CdS has been extensively studied as a photocatalyst for the degradation of organic dyes, but its usage in hydrogen production studies is rather limited due to its photocorrosive nature.[12,13]

Designing CdS nanomaterials with matching redox potentials for the aforementioned applications is of great interest in material science. Although a variety of techniques such as thermal evaporation, hydrothermal method, chemical vapor deposition process, template method, thermal decomposition method and solvothermal process are reported for the preparation of CdS quantum dots, many of them demand complicated procedures, inert conditions and longer reaction times and use of costly surfactants to produce CdS with different morphologies.[14–19] In this context, combustion synthesis with less energy payback time (a key parameter in life cycle analyses of solar energy materials and devices) is receiving more attention, especially for synthesis of oxides.[20–22]

However, application of combustion for the synthesis of metal chalcogenides is not fully explored. To the best of our knowledge, this is probably the first attempt of metal sulphide synthesis by using solution combustion method without maintaining any inert conditions. This study reports a facile synthesis of C and N doped CdS nanomaterials. Synthesized CdS nanomaterials have been tested for the visible light-driven hydrogen production from water splitting.

*For correspondence

2. Experimental

Cadmium nitrate tetrahydrate and thiourea were purchased from Merck and used as received. Required quantities of precursors were calculated based on the oxidant/fuel (O/F) ratio obtained by using propellant theory. In a typical synthesis, aqueous solutions of cadmium nitrate and thiourea were mixed to form a homogeneous solution. Dehydration followed by combustion in a preheated furnace at 300°C resulted the product in a few minutes. Different oxidant/fuel (O/F) ratios (1, 2, 3, 4 and 10) have been studied and the resulting CdS samples were labelled as CdS (1), CdS (2), CdS (3), CdS (4) and CdS (10), respectively. Since costly surfactants, capping agents and inert conditions are not used in this synthesis, it is a very cost-effective method. Moreover, the samples can be used without any post-treatments such as washing and calcination.

2.1 *Characterization*

Cadmium sulphide samples were characterized to examine its structural, morphological, and optical properties. Phase purity and crystallinity of the as-synthesized CdS samples were obtained from powder X-ray diffraction (PXRD) patterns recorded on a PANalytical X'pert Pro powder X-ray diffractometer with a step size of 0.02 at a scan rate of 0.50 min^{-1} using Cu-Kα (1.54 Å) radiation and Ni filter. Transmission electron microscopic image of the CdS(2) sample was recorded at an operating voltage of 200 kV and the sample was placed on a copper grid (TECNAI G-2 with EDS model), whereas, diffuse UV-Vis reflectance spectra of the prepared samples were collected using Shimadzu UV-Vis spectrophotometer (UV-3600) with spectral grade $BaSO_4$ as reference. X-ray photoelectron spectroscopic study was performed on Axis Ultra instrument under ultra-high vacuum condition (<10^{-8} Torr) and by using a monochromatic Al Kα X-ray source (1486.6 eV). Raman spectra of the as-synthesized samples were carried out with a dispersive Raman spectroscope (Bruker Senterra).

2.2 *Photocatalytic reactions*

Photocatalytic water splitting under simulated visible light radiation was performed in a quartz round-bottomed flask containing 100 mL water and 100 mg of the catalyst. The study was carried out in the presence of 1 M Na_2S and 1 M Na_2SO_3 as the sacrificial reagents. Before addition of CdS catalyst, N_2 was bubbled for 30 min, followed by evacuation for 15 min to remove the dissolved gases. After addition of the CdS catalyst, the solution was stirred in dark for 30 min in order to facilitate the adsorption of water molecules on the CdS surface. It is worth mentioning that there is no appreciable reaction in the dark. All the studies were carried out under simulated visible light radiation with light intensity around 800–900 W/m^2, as measured by Newport power meter. Hydrogen produced in the reaction was analysed by using a Shimadzu gas chromatography (GC-2014) equipped with TCD detector, packed column and N_2 carrier gas. Every hour, a 500 μl hydrogen gas was collected in a gas tight syringe (Hamilton) and injected into the GC. Calibration curve has been drawn by taking different volumes of pure H_2 and injecting into the GC. The area under the evolved H_2 gas was compared with the area under the calibration curve and quantified in terms of μmol.

3. Results and Discussion

3.1 *Powder X-ray diffraction*

Combustion-synthesized cadmium sulphide samples with varying O/F ratios from 1 to 10 were characterized by PXRD to identify phase purity and crystallite size. As shown in figure 1, except in the case of O/F ratio 1, pure CdS was observed for other ratios. CdS (1) with more intense diffraction peaks at d-spacing of 2.7, 2.4 and 1.7 Å with corresponding planes (111), (200) and (220) confirms the existence of CdO. This can be attributed to insufficient fuel, thiourea. CdS (2) shows major peaks at 2θ; = 28.2°, 24.8°, 43.7°, 26.5°

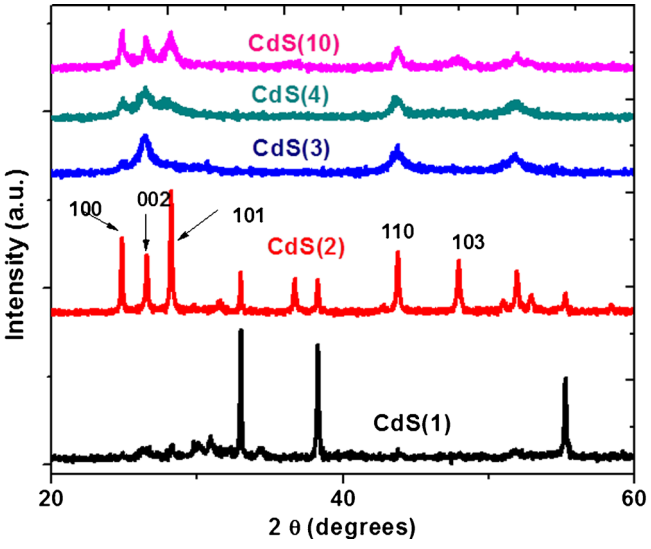

Figure 1. Powder X-ray diffraction patterns of combustion-synthesized cadmium sulphide samples.

and 47.9° corresponding to 101, 100, 110, 002 and 103 planes with the corresponding d-spacing values are 3.6, 3.4, 3.2, 2.1 and 1.9 Å representing hexagonal CdS. From figure 1, it was observed that CdS (3) and CdS(4) also have diffraction peaks corresponding to the hexagonal phase. However, in the case of CdS (3), the peaks corresponding to (101), (100) and (002) planes seems overlapped due to the small crystallite size (around 14 nm). However, for CdS(4) and CdS(10), these peaks are distinguishable due to large crystallite size (around 25 nm).

Generally, broadening of diffraction peak may be due to one of the following factors such as micro strain (deformations of the lattice), crystalline faults (extended defects), crystalline size and domain size distribution.[23–25] Average crystallite sizes of the CdS samples calculated by using Scherrer formula was found to be 58, 70, 14, 20 and 25 nm for CdS (1), CdS (2), CdS (3), CdS (4) and CdS (10), respectively. Larger crystallite size in case of CdS (2) may be explained on the basis of optimum O/F ratio, which facilitates the combustion and provides high temperatures for crystal growth.[13]

3.2 *Transmission electron microscopy*

In order to confirm the phase and crystallite size, TEM studies were carried out for all the CdS samples. Figure 2 shows TEM image of best active CdS(2) sample, whereas TEM images of all the remaining CdS samples are given in supporting information (figure S1 to S4). From figure 2a, it is clear that CdS(2) sample consists of some irregular-shaped crystalline nanoparticles. Particle size was found to be around 70 nm which is in good agreement with the PXRD results. Selected area electron diffraction pattern (figure 2b) with d-spacing corresponding to the planes (100), (002), (103) and (110) confirmed the hexagonal CdS phase which is also in good agreement with the XRD results. From figure S1 to S4, it is clear that CdS(1), CdS(3), CdS(4) and CdS(10) samples have several nanoparticles with almost spherical morphology. Thus, the best activity of CdS(2) might be attributed to its good crystalline nature as confirmed by XRD rather than its morphology.

3.3 *Diffuse UV-Vis spectroscopy*

It is well-known that CdS is a direct band gap semiconductor with a band gap energy of 2.4 eV. A red shift in the absorption due to C and N doping was recognized from absorption spectra of the combustion-synthesized CdS samples (figure 3). Band gap energies of CdS (1), CdS (2), CdS (3), CdS (4) and CdS (10) samples were found to be 2.0, 2.2, 2.3, 2.4 and 2.4 eV, respectively. Band gap energy of 2.0 eV in case of CdS (1) could be attributed to the C and N doped CdO (band gap of CdO is 2.16 eV). Among CdS (2), CdS (3), CdS (4) and CdS (10) samples, CdS (2) was found to have a low band gap of 2.2 eV, probably due to more C and N doping compared to the rest of the samples and with increasing O/F ratio from 3 to 10 band gap again increased to the original value of 2.4 eV due to fuel rich conditions, which hindered proper combustion. Higher C and N doping in CdS(2) sample compared to the other CdS samples can be explained as follows: In general, O/F ratio of 1 is the optimum ratio for the combustion synthesis of materials. However, in the present synthesis, O/F = 2 is the optimum ratio in such a way that it is small enough to produce the sulphide phase at normal atmospheric conditions as well as to produce proper

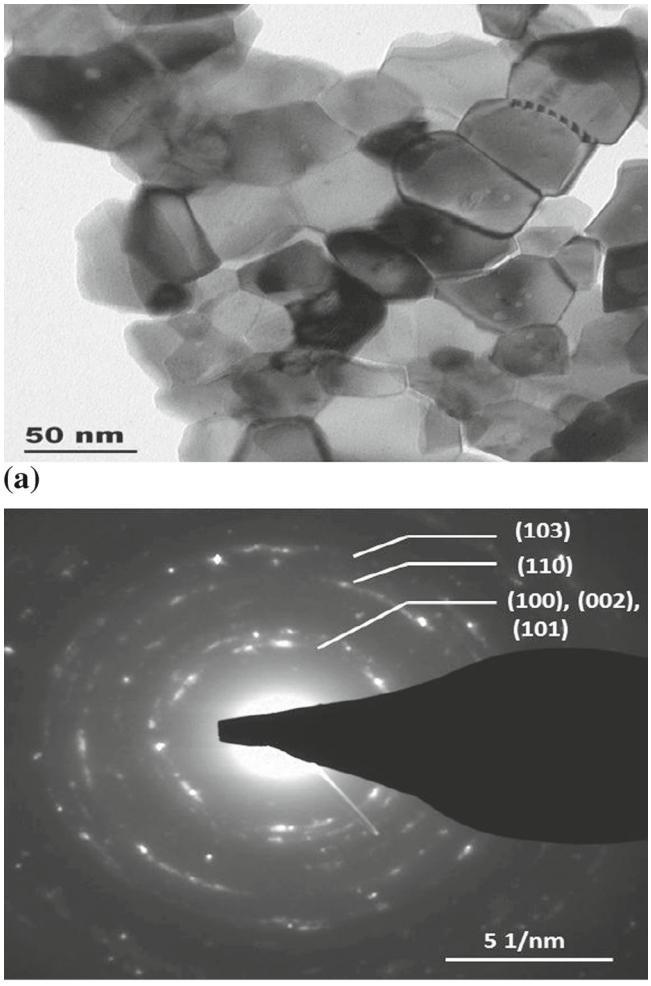

Figure 2. **(a)** TEM image of the best active CdS (2) sample which shows irregular-shaped nanoparticles. (**b**) Selected area electron diffraction pattern of the CdS(2) sample showing different planes corresponding to the hexagonal CdS phase.

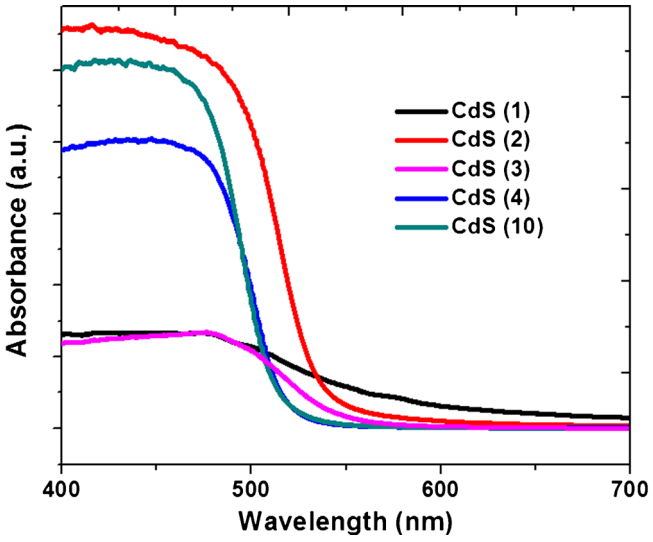

Figure 3. Diffuse reflectance UV-Vis spectra of combustion-synthesized CdS samples.

combustion conditions with more evolved gases. Thus, in case of CdS(2) sample, optimum O/F ratio has been achieved that might facilitate proper combustion, which in turn enables proper C and N doping into the CdS matrix.

3.4 *X-ray photoelectron spectroscopy*

In order to confirm the presence of C and N doping, XPS study of CdS (2) sample was carried out and the spectra are shown in figure 4. As seen in figure 4a, Cd (3d) spectra showed two peaks centered at 405.2 and 411.9 eV, characteristic of Cd $3d_{5/2}$ and Cd $3d_{3/2}$, respectively.[26–29] Whereas the S 2p peak observed at 161.5 eV and 162.7 eV as shown in figure 4b inferred the existence of sulphides. Absence of peaks centered at 165 and 170 eV reveals the existence of sulphur in non-oxidized form.

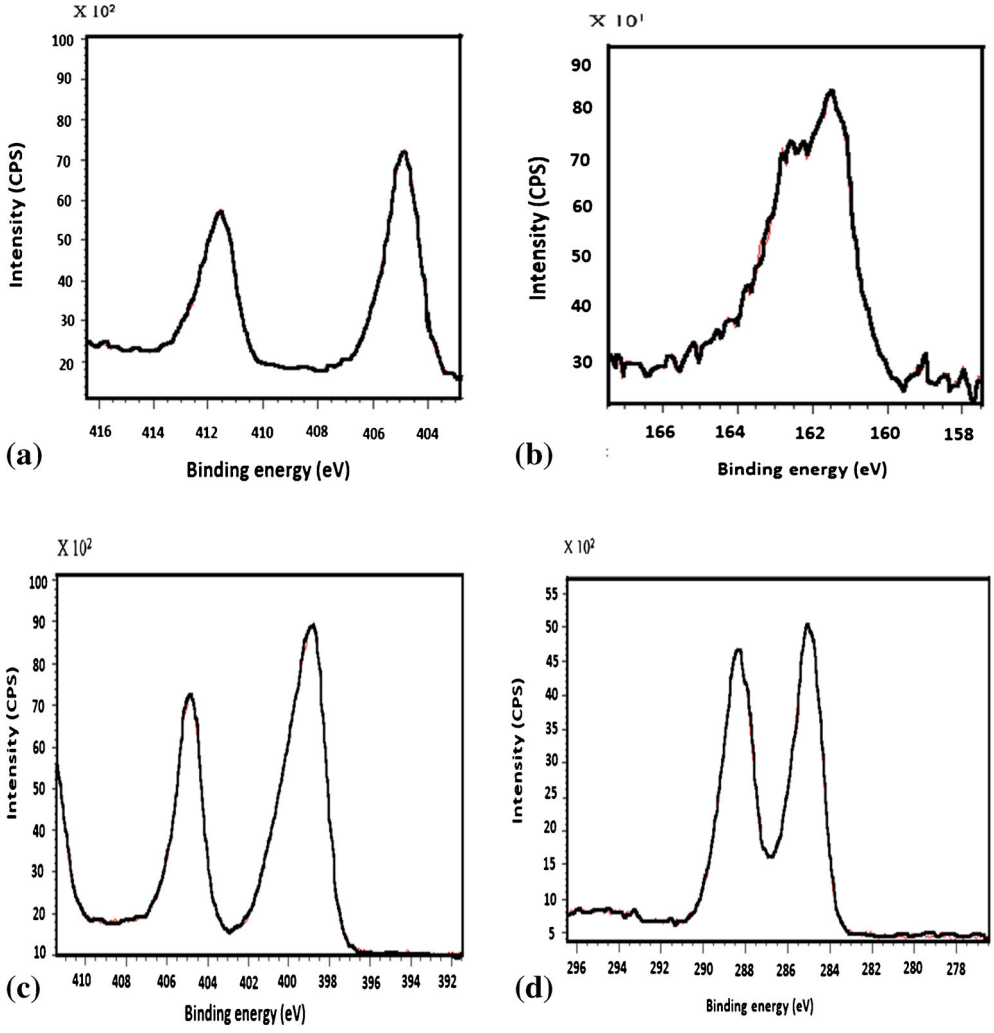

Figure 4. XPS spectra of (**a**) Cd 3d core levels, (**b**) S 2p core levels, (**c**) C 1s core levels, (**d**) N 1s core levels of the best active CdS (2) sample.

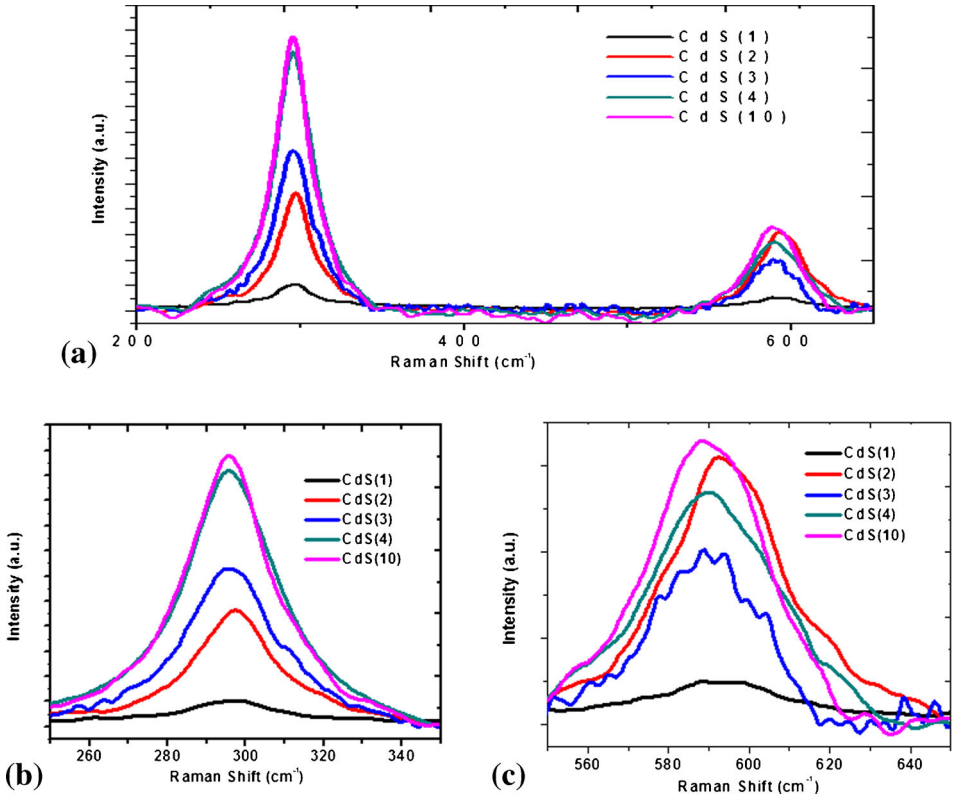

Figure 5. (**a**) Raman spectra of CdS samples. (**b**) Enlarged view of A11LO phonon mode of CdS samples. (**c**) Enlarged view of A1 2LO phonon mode of CdS samples.

Presence of C as a dopant was clearly shown by the peaks at 285 and 289 eV in the deconvoluted C 1s spectra as represented in figure 4c. The former peak might occur due to the aliphatic carbon, whereas the latter one occurred due to the C bonded with O and/or S, either with a double bond or two single bonds.[30] Similarly, evidence for nitrogen doping was provided from the N (1s) spectra that showed two peaks at 399.7 and 405 eV(figure 4d). Literature data confirmed that binding energy of the N 1s was very sensitive to the chemical environment of nitrogen and it varies from 396 to 408 eV.[31] The peaks observed at 399.7 eV correspond to the terminally bonded well-screened molecular nitrogen (γ-N_2), whereas, the 405 eV peak might occur due to terminally bonded poorly screened molecular nitrogen (γ-N_2).[32]

3.5 *Raman spectra*

Hexagonal CdS is one of the simple uniaxial structures that can be analysed by Raman scattering phenomena.[33] Figure 5a presents Raman spectra of the synthesized CdS samples, whereas figure 5b and c showed enlarged views of the A11LO and AL2LO phonon modes of CdS, respectively. It represents two distinct Raman bands in the spectral region of 200 to 700 cm^{-1}. Raman bands at 299 and 600 cm^{-1} correspond to the A1 1LO (longitudinal optical) and A1 2LO phonons, respectively and the intensity of A1 2LO phonon at 600 cm^{-1} was lower compared to the intensity of A1 1LO mode at 299 cm^{-1}.[34–38] As seen clearly from figure 5b and c that with increasing O/F ratio, the peak shifted to lower

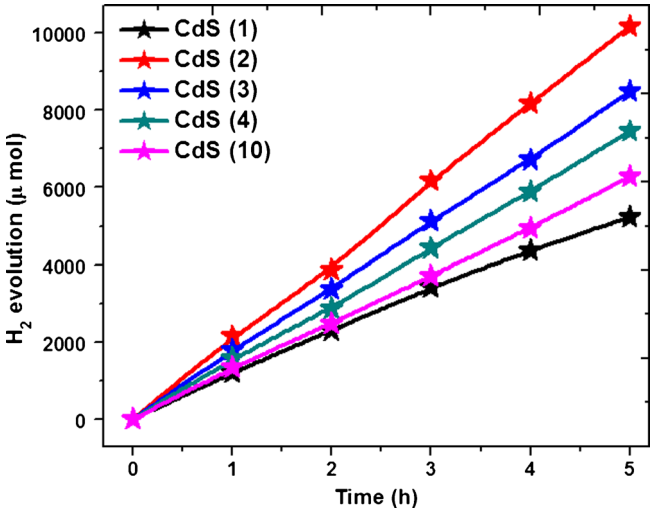

Figure 6. Photocatalytic H_2 evolution profiles from splitting of water containing Na_2S and Na_2SO_3 sacrificial reagents under visible light in the presence of different CdS samples.

frequency region and full width half maxima (FWHM) increased due to the difference in the crystalline sizes.

3.6 *Photocatalytic studies*

Since CdS is well-known for its visible light activity and also the *in situ* doping of C and N into the CdS has been confirmed, visible light activity of the CdS was tested for hydrogen production from water. Although CdS has good absorption in the visible region, its photocorrosive nature limits its application in H_2 production.[39] In order to reduce photocorrosion of CdS and to prevent recombination of excitons, water containing 1M Na_2S and 1M Na_2SO_3 as sacrificial reagents were used. These sacrificial reagents may interact with the holes that prevent photocorrosion of CdS catalyst.[39] During the photocatalytic reaction, for every 1 h, H_2 gas was collected by using a gas tight syringe and analysed by gas chromatography. Typical chromatogram observed is shown in figure S5 (supporting information). H_2 production studies were carried out with all the CdS samples and the typical results shown in figure 6 confirmed the formation of 1215, 2135, 1800, 1590 and 1345 μ mol/h of hydrogen, respectively for CdS (1), CdS (2), CdS (3), CdS (4) and CdS (10). These results confirmed that the highest hydrogen evolution was achieved for CdS (2). In order to assess the stability of CdS(2) photocatalyst for hydrogen production, the activity was monitored for 25 h by evacuating the reactor after every 5 h and the results are shown in figure 7. After 25 h, decrease in H_2 production was found to be approximately 10% confirming the reasonable stability of the catalyst. The best activity of CdS(2) can be attributed to the higher crystallinity and low band gap, due to which it has the best absorption in the visible region.

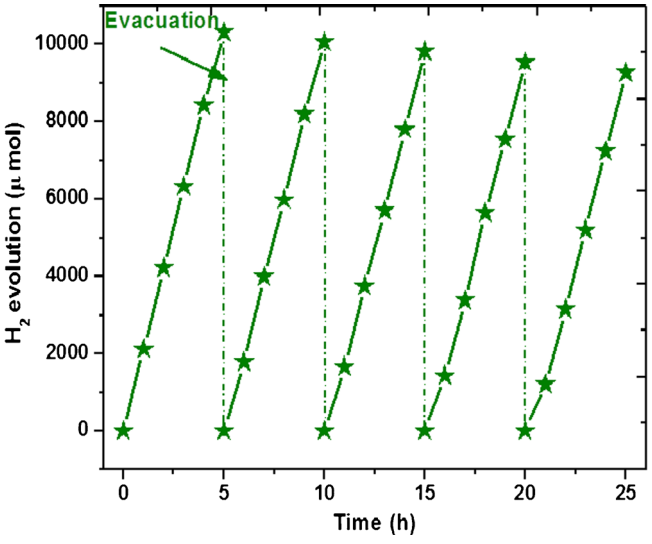

Figure 7. H_2 evolution profiles from water containing Na_2S and Na_2SO_3 sacrificial agents in the presence of CdS (2) (five runs in a continuous reaction are shown).

4. Conclusions

A highly efficient synthesis of C and N doped nanocrystalline CdS has been reported by using solution combustion synthesis without using any surfactant. Variation of O/F ratio between 1 and 10 revealed that the sample synthesized at O/F ratio of 2 had the best photocatalytic activity. Efficient hydrogen production of 2120 μmol/h from water containing 1 M Na_2S and 1M Na_2SO_3 as sacrificial agents under visible light irradiation validated the synthesis approach. The best activity of CdS(2) may be attributed to the good absorption in the visible region, resistance to photocorrosion and prevention of excition recombination by the dopant energy levels.

Supplementary information

TEM images of the CdS(1), CdS(3), CdS(4) and CdS(10) samples and the corresponding discussion is provided in the supplementary information. Gas chromatogram observed during the H_2 analysis was included in the revised manuscript.

Acknowledgement

Ms. Daya Mani would like to thank MHRD, India for UGC-JRF fellowship.

References

1. Cox P M, Betts R A, Jones C D, Spall S A and Totterdell I J 2000 *Nature* **408** 184
2. Coelho B, Oliveira A C and Mendes A 2010 *Energy Environ. Sci.* **3** 1398
3. Jacobson M Z, Colella W G and Golden D M 2005 *Science* **308** 1901
4. Jain I P 2009 *Int. J. Hydrogen Energ.* **34** 7368
5. Li C and Fang H H P 2007 *Crit. Rev. Env. Sci. Technol.* **37** 1
6. Holladay J D, Hu J, King D L and Wang Y 2009 *Catal. Today* **139** 244
7. Onuki K, Kubo S, Terada A, Sakaba N and Hino R 2009 *Energy Environ. Sci.* **2** 491

8. Wang X, Maeda K, Thomas A, Takanabe K, Xin G, Carlsson J M, Domen K and Antonietti M 2009 *Nat. Mater.* **8** 76
9. Pan H, Poh C K, Zhu Y W, Xing G C, Chin K C, Feng Y P, Lin J Y, Sow C H, Ji W and Wee A T S 2008 *J. Phys. Chem. C* **112** 11227
10. Lin Y F, Song J H, Ding Y, Lu S Y and Wang Z L 2008 *Adv. Mater.* **20** 3127
11. Shen G Z, Cho J H, Yoo J K, Yi G C and Lee C J 2005 *J. Phys. Chem. B* **109** 9294
12. Apte S K, Garaje S N, Mane G P, Vinu A, Naik S D, Amalnerkar D P and Kale B B 2011 *Small* **7** 957
13. Bao N, Shen L, Takata T, Domen K, Gupta A, Yanagisawa K and Grimes C A 2007 *J. Phys. Chem. C* **111** 17527
14. Wang Q Q, Xu G and Han G R 2006 *Crsyt. Growth Des.* **6** 1776
15. Thiruvengadathan R and Regev O 2005 *Chem. Mater.* **17** 3281
16. Jianzhong J, Yane H, Leping W, Zhe C, Zhenggang C and Philip G J 2013 *Chem. Commun.* **49** 1912
17. Bo Z, Weifeng Y, Cunping H, Qunjie X and Qiang W 2013 *Int. J. Hydrogen Energ.* **38** 7224
18. Jum S J, Upendra A J and Jae S L 2007 *J. Phys. Chem. C* **111** 13280
19. Jiaguo Y, Yanfang Y and Bei C 2012 *RSC Adv.* **2** 11829
20. Rajeshwar K and Tacconi N R D 2009 *Chem. Soc. Rev.* **38** 1984
21. Guo X, Mao D, Wang S, Wu G and Lu G 2009 *Catal. Commun.* **10** 1661
22. Zhang Z, Wang W, Shang M and Yin W 2010 *Catal. Commun.* **11** 982
23. Klug H P and Alexander L E 1954 *X-ray diffraction procedures for polycrystalline and amorphous materials* 1st ed., Chapter 9 (New York: Wiley)
24. Shen L, Bao N, Yanagisawa K, Domen K, Gupta A and Grimes C A 2006 *Nanotechnology* **17** 5117
25. Shen L, Bao N, Yanagisaw K, Zheng Y, Domen K, Gupta A and Grimes C A 2007 *J. Phys. Chem. C* **111** 7280
26. Zhai T, Fang X, Bando Y, Liao Q, Xu X, Zeng H, Ma Y, Yao J and Golberg D 2009 *ACS Nano.* **3** 949
27. Xiong S, Zhang X and Qian Y 2009 *Cryst. Growth Des.* **9** 5259
28. Katari J E B, Colvin V L and Alivisatos A P 1994 *J. Phys. Chem.* **98** 4109
29. Wang D, Li D, Guo L, Fu F, Zhang Z and Wei Q 2009 *J. Phys. Chem. C* **113** 5984
30. Li Y, Hwang D-S, Lee N H and Kim S-J 2005 *Chem. Phys. Lett.* **404** 25
31. Moulder J F, Stickle W F, Sobol P E, Bomben K D and Chastain J 1992 *Handbook of X-ray electron spectroscopy* Eden Prairie (MN: Perkin-Elmer Corp.)
32. Shinn N D and Tsang K L 1991 *J. Vac. Sci. Technol. A* **9** 1558
33. Nusimovici M A and Birman J L 1967 *Phys. Rev.* **156** 925
34. Arguello C A, Rousseau D L and Porto S P S 1969 *Phys. Rev.* **181** 1351
35. Tell B, Damen T C and Porto S P S 1966 *Phys. Rev.* **144** 771
36. Pan A, Liu R, Yang Q, Zhu Y, Yang G, Zou B and Chen K 2005 *J. Phys. Chem. B* **109** 24268
37. Fan H M, Ni Z H, Feng Y P, Fan X F, Kuo J L, Shen Z X and Zou B S 2007 *Appl. Phys. Lett.* **91** 171911
38. Yamamoto A, Endo H, Matsuura N, Ishizumi A and Kanemitsu Y 2009 *Phys. Stat. Sol. C* **6** 197
39. Muruganandham M, Ramakrishnan A, Kusumotob Y and Sillanpaa M 2010 *Phys. Chem. Chem. Phys.* **12** 14677